




Article

Flotation Behavior and Synergistic Mechanism of Benzohydroxamic Acid and Sodium Butyl-Xanthate as Combined Collectors for Malachite Beneficiation

Chenyang Zhang ^{1,2}, Qiqi Zhou ¹, Bingxuan An ¹, Tong Yue ¹ , Shengda Chen ¹, Mengfei Liu ¹, Jianyong He ¹ , Jianyu Zhu ¹ , Daixiong Chen ², Bo Hu ^{3,*} and Wei Sun ^{1,*}

- ¹ Key Laboratory of Hunan Province for Clean and Efficient Utilization of Strategic Calcium-Containing Mineral Resources, School of Minerals Processing and Bioengineering, Central South University, Changsha 410083, China; zhangchenyang@csu.edu.cn (C.Z.); qiqizhou@csu.edu.cn (Q.Z.); bingxuan_an@163.com (B.A.); yuetong@csu.edu.cn (T.Y.); 185611030@csu.edu.cn (S.C.); liumengfei0813@163.com (M.L.); hjy2016@csu.edu.cn (J.H.); zhujy@csu.edu.cn (J.Z.)
- ² Key Laboratory of Hunan Province for Comprehensive Utilization of Complex Copper-Lead Zinc Associated Metal Resources, Hunan Research Institute for Nonferrous Metals, Changsha 410100, China; chendaixiong888@163.com
- ³ School of Resources and Environmental Engineering, Wuhan University of Science and Technology, Wuhan 430081, China
- * Correspondence: hubo_hrinm@163.com (B.H.); sunmenghu@csu.edu.cn (W.S.); Tel.: +86-0731-8501-1193 (B.H.); +86-0731-8883-0482 (W.S.)



Citation: Zhang, C.; Zhou, Q.; An, B.; Yue, T.; Chen, S.; Liu, M.; He, J.; Zhu, J.; Chen, D.; Hu, B.; et al. Flotation Behavior and Synergistic Mechanism of Benzohydroxamic Acid and Sodium Butyl-Xanthate as Combined Collectors for Malachite Beneficiation. *Minerals* **2021**, *11*, 59. <https://doi.org/10.3390/min11010059>

Received: 25 November 2020

Accepted: 2 January 2021

Published: 10 January 2021

Publisher's Note: MDPI stays neutral with regard to jurisdictional claims in published maps and institutional affiliations.



Copyright: © 2021 by the authors. Licensee MDPI, Basel, Switzerland. This article is an open access article distributed under the terms and conditions of the Creative Commons Attribution (CC BY) license (<https://creativecommons.org/licenses/by/4.0/>).

Abstract: Sulfuration flotation is the most widely used technology in malachite beneficiation. However, the inhomogeneity of malachite surfaces usually results in a non-uniform sulfuration surface. The motivation of this work is attempt to adopt different functional combination collectors to enhance the sulfuration flotation of malachite. Accordingly, the flotation behaviors and adsorption mechanisms of benzohydroxamic acid (BHA) and sodium butyl-xanthate (SBX) on the surface of malachite were systematically investigated using flotation tests, zeta-potential measurements, Fourier-transform infrared (FTIR) spectroscopy, Raman spectroscopy, and first-principle calculations. The test results of vulcanization flotation showed that the combined collectors of SBX with BHA possessed a higher recovery than only using SBX by 20%, indicating that there may be a synergistic effect between BHA and SBX. The IR and Raman spectroscopy demonstrated that both BHA and SBX could chemically adsorb onto the malachite surface. The density functional theory (DFT) calculation results further indicated that the combined adsorption energy of BHA and SBX was much lower than that of only BHA or SBX, which confirmed the synergistic effects of BHA and SBX on the malachite surface. This work may shed new light on the design and development of more efficient combined flotation reagents.

Keywords: malachite; flotation; combined collectors; synergistic effect; DFT calculations

1. Introduction

As an important non-ferrous metal, copper mainly exists in the form of sulfide [1–4]. With the decrease of copper sulfide resources, the utilization of oxidized copper ore has been paid more and more attention. Malachite is the most representative of oxidized copper minerals [5,6]. It belongs to the category of monoclinic systems [7]. Its crystal structure is columnar and needle-like, and it is a mineral possessing a layered pore structure, concentric layer structure, and radial fiber shape. Malachite occurs in the oxidation zone of copper sulfide ore. It is a secondary mineral produced by weathering, possessing the characteristics of high hydrophilicity and complex structure [8–10].

Flotation is one of the most important methods for the beneficiation of oxidized copper minerals [11–13]. The flotation of copper oxide ore can mainly be divided into

direct flotation and sulfuration flotation. Advanced xanthate, fatty acids, and hydroxamic acids are usually used as collectors in the direct flotation [14]. However, these collectors have not been widely used in industrial applications due to their inferior selectivity and high cost. Currently, sulfuration flotation is the most extensively used method for flotation of copper oxide ore in the industry [15–21]. The sulfuration flotation method is a method in which initially oxidized minerals are pre-vulcanized by a soluble vulcanizing agent, and subsequently, flotation is performed using a collector of the vulcanized ore [22]. However, there are still some problems in sulfuration flotation, including large dosage of reagents, incomplete vulcanization, and instability of sulfide film.

In order to avoid these problems, researchers usually used activators to strengthen sulfuration and improve the flotation efficiency. For example, Liu et al. used sodium chloride to enhance the sulfidation flotation of cerussite and found that sodium chloride can make the surface of the cerussite form more lead sulfide species and improve the sulfidation flotation performance [23]. Feng et al. [6] used ethylenediamine to modify the surface of malachite to improve the sulfuration flotation. The results showed that ethylenediamine-modified malachite not only increases the contents of copper sulfide species on the malachite surface, but also enhances the reactivity of the vulcanized product, thus improving malachite recovery. Alternatively, the use of mixed reagents as collectors could also possibly improve the flotation efficiency based on the synergistic effects between the agents. In fact, the combined collectors have been widely used in flotation and have achieved good results. For example, Gao et al. [24] found that the mixed use of C₁₂₋₁₆COONa and MES (sodium fatty acid methyl ester sulfonate) has high selectivity for the flotation of scheelite in calcite and fluorite. The mixed cationic collector dodecyl ammonium chloride (DTAC) and anionic collector sodium oleate (NaOL) have high selectivity for the flotation of spodumene from feldspar [25]. Recently, Sun et al. also reported the synergistic enhancement effect of sodium butyl xanthate (NaBX) and dodecylamine (DDA) as a combined collector on the sulfidizing flotation of copper oxide [26]. As is well known, the inhomogeneity of malachite surfaces usually results in non-uniform sulfuration surfaces in sulfuration flotation, which could be approximately divided into a sulfurized zone and an unsulfurized zone. Thus, the motivation of this work is an attempt to adopt different functional combination collectors to enhance the sulfuration flotation of malachite based on the basic assumption that the sulfide mineral collector (sodium butyl-xanthate) could interact well with the sulfurized zone and the oxide mineral collector (benzohydroxamic acid) could interact well with the unsulfurized zone.

However, traditional experimental characterizations are not sufficient to accurately describe the involved micro-processes. Owing to the rapid developments in theoretical and computational chemistry, more effective tools, such as quantum chemistry calculations, can be used to better understand the adsorption mechanisms of flotation reagents on target minerals. For example, Lebernegg et al. selected the surface of malachite (201) to conduct related studies using quantum chemical calculations and demonstrated that this surface is the dissociation surface of a malachite crystal with a complete structure [9]. Wu et al. [10] studied the activation mechanism of ammonium ion on malachite sulfuration using density functional theory (DFT) calculations. It was found that after the ammonium ion activated sulfidation, the Cu 3d orbital peak was closer to the Fermi level and was characterized by a stronger peak value, thus enhancing the sulfuration of malachite.

Accordingly, the synergistic collection mechanism of malachite by BHA and SBX was examined using a combination of theory and experiments in this work. The optimal dosage ratio of BHA and SBX was obtained with flotation experiments. The flotation behaviors and micro-mechanisms of both reagents on the surface of malachite were investigated by zeta-potential measurements, Fourier-transform infrared (FTIR) spectroscopy, Raman spectroscopy, and first-principle calculations. This work might shed new light on the design and development of more efficient combined flotation reagents based on the consideration of the surface micro-structures.

2. Materials and Methods

2.1. Materials and Reagents

For the experiment, before crushing by a jaw crusher, the larger malachite was smashed into small pieces of about 1.5 cm, and was then put into the pure mineral jaw crusher to crush the small particles to about 2 mm. The 2 mm particles were put into a pure mineral ceramic ball grinding tank for grinding. The ore samples were successively sifted through a 200-mesh and 400-mesh standard sieve; then, a mineral sample with a particle size of 38–74 μm was obtained. The X-ray diffraction (XRD) analysis results of the pure mineral of malachite used in the experiment were as displayed in Figure 1; the malachite sample had over 98% of malachite, so the sample was pure enough for the following research.

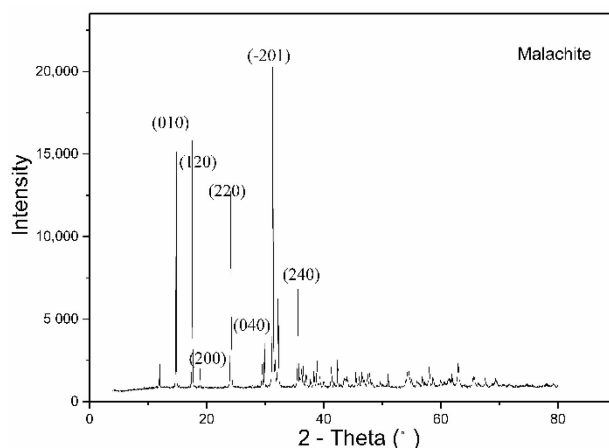


Figure 1. X-ray diffraction (XRD) pattern of the malachite sample.

Analytical grade sodium sulfide (Na_2S), sodium chemical pure butyl xanthate (SBX), benzohydroxamic acid (BHA), terpenic oil (foaming agent), sodium hydrate (NaOH), hydrochloric acid (HCl), and deionized water were used in this study. It is worth noting that the collector, SBX, and sodium sulfide hydrate used in the experiment must be stringently prepared and used immediately to ensure the accuracy of the experimental results. BHA is an O-O type chelate collector. As an oxide mineral collector, it has the advantages of high selectivity, low toxicity, and high efficiency. SBX is the most commonly used flotation collector of sulfide minerals [27]. It typically exists as light yellow particles or powder with a pungent odor.

2.2. Methodology

2.2.1. Micro-Flotation

The mineral flotation experiment of malachite was conducted on an XFGII-type hanging-tank flotation machine. The volume of the flotation tank was 40 mL, and the spindle speed was 1500 rpm. Each time, 2 g of the mineral was weighed (the error was controlled within 0.001 g) and mixed with 35 mL of deionized water, and the pH was adjusted to 9.5 in 2 min by NaOH and HCl (it should be mentioned that a typical pH value of 9.5 was chosen in this study, considering that the separation of malachite minerals are often in an alkaline pulp environment in most plants [26]). Subsequently, the vulcanizing agent, collector, and foaming agent (the dosage of terpineol oil was 40 mg/L [17]) were added in order, and the specific flotation process is illustrated in Figure 2. Following the completion of the flotation, the foam product and the product in the tank were filtered and dried to determine the flotation recovery. To obtain accurate and reliable results, each set of experiments was conducted thrice and the average values were taken.

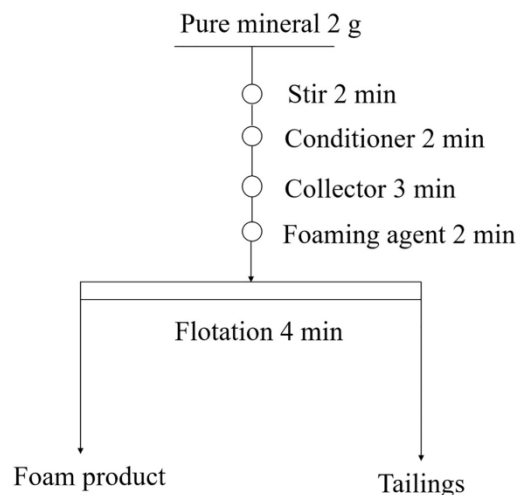


Figure 2. Flowchart of the flotation tests.

2.2.2. Zeta-Potential Measurements

Zeta potential is the electric potential in the interfacial double layer at the location of the slipping plane relative to a point in the bulk fluid away from the interface [28]. A Malvern Zeta-sizer Nano machine (Malvern Panalytical, Malvern, UK) was used to measure the zeta potential at 20 °C. A supernatant of malachite particles was prepared for the zeta-potential measurement. KNO_3 was used as an ordinary background electrolyte [3]. The mineral was added into the electrolyte solution and placed on a magnetic stirrer for stirring, and the pH value was adjusted using 0.1 mol/L HCl or 0.1 mol/L NaOH solution. Then, the flotation reagent was added according to the flotation process under the determined pH value, and the reagent dosage was the reagent dosage for the optimal recovery. The suspension was placed in a magnetic agitator for 5 min to disperse the suspended particles adequately, and was then precipitated for 5 min. Subsequently, to prevent the formation of bubbles, the supernatant was slowly injected into a test cell with a syringe for conducting the tests.

2.2.3. Fourier-Transform Infrared Spectroscopy

Fourier-transform infrared (FTIR) adsorption spectroscopy has been used as a quantitative analysis method for some minerals [29]. The FTIR spectra of a batch of malachite samples were measured by a Germany Fourier-Transform Infrared Spectroscopy (FTIR) Vertex 80v (Germany Bruker, Karlsruhe, Germany) following the flotation test processing procedures. The samples were ground to less than 5 microns to obtain the test samples. Then, 2 g of malachite were added to 40 mL deionized water and the pH was adjusted to 9.5. According to the flotation process, the flotation reagents were added in sequence, and then the samples were filtered and washed with deionized water three times before drying. The transmission spectrum of malachite used 10% malachite samples and 90% potassium bromide in a vacuum cell so that one could see more details from the spectrum. The infrared spectra of the samples were recorded with an FTIR spectrometer at room temperature (25 ± 1 °C) in a range from 400 to 4000 cm^{-1} .

2.2.4. Raman Spectroscopy

Unlike FTIR, Raman spectroscopy probes the vibrational spectrum by using inelastic scattering. In many cases, Raman spectroscopy and FTIR spectroscopy are complementary [30]. Raman spectroscopy can reflect the structure and composition of molecules [31], the reactions of symmetric structures (such as C–C), and the skeletons of the molecules. A Raman spectroscopy test does not require pre-treatment of the sample, and a mineral can be directly tested. Micro-analysis of minerals with micro-scale resolution and ultra-high sensitivity can be performed with trace minerals, even with trace impurities [32].

The Renishaw inVia confocal Raman spectrometer (Renishaw, Gloucestershire, UK) was used in the experiment with a 532 nm laser emitter. The room temperature was maintained at 25 °C and the humidity was 30%. The samples were ground to less than 5 microns to obtain the test samples. Then, 2 g of malachite were added to 40 mL deionized water, and the pH was adjusted to 9.5. According to the flotation process, the flotation reagents were added in sequence, and then the samples were filtered and washed with deionized water three times before drying. Before each start-up experiment, the silicon wafer was calibrated to ensure that the built-in silicon peak was in the range of 520–520.5 cm^{-1} . Before the beginning of each experiment, the percentage of laser power output was measured, and then the resolution and signal-to-noise ratio were adjusted to obtain accurate and repeatable experimental spectral results. A small amount of sample was placed on the slide, and then the surface of the sample was flattened. The slides were placed under a 50 \times objective lens, and the Raman spectroscopy tests were performed.

2.2.5. Computational Details

A periodic model of bulk phase was built from the XRD crystal structure obtained from the American Mineralogist Crystal Structure Database [33]. All the periodic calculations were performed by the CASTEP [34] module in Materials Studio 2017 (MS 2017). A previous study by Wu et al. [10] indicated that generalized gradient approximation (GGA)-PW91 could be used to obtain reasonable lattice constants of the malachite unit cell that are relatively close to the experimental ones. Hence, the electronic exchange–correlation energy was treated within the generalized gradient approximation (GGA) by using the PW91 gradient correction functional with an appropriate cut-off energy of 351 eV [35]. The ultrasoft pseudopotential (Ultrasoft) of the PW91 base group was used to describe the interaction between the ionic core and the valence electron [36].

All the periodic optimization calculations were performed, allowing atomic positions, lattice vectors, and angles to relax within a constrained total volume based on a plane-wave basis set. A fine k-point mesh with Monkhorst-Pack k-point grids ($2 \times 2 \times 1$) was used to provide a precise estimation of the crystal structure of malachite. In the self-consistent field calculation, the Pulay density mixing method was used, and the convergence precision was set as 1×10^{-6} eV/atom. In all the optimization calculations, using BFGS algorithm, the convergence criteria of the energy, the maximum force, the maximum stress, and the maximum atomic displacement were set as 2×10^{-5} eV/atom, 0.05 eV/Å, 0.1 GPa, and 0.002 Å, respectively.

The quantum chemistry calculations of BHA and SBX were performed with the Gaussian 09 (version D.01) software based on the B3LYP method with the cc-pVDZ basis set [37]. The highest occupied molecular orbital (HOMO) and the lowest unoccupied molecular orbital (LUMO) were rendered to demonstrate the reactivity of the studied molecule.

3. Results and Discussion

3.1. Micro-Flotation Tests

Figure 3a,b shows the malachite recovery as a function with respect to the dosage of Na_2S and collectors. In the absence of Na_2S , the recovery of malachite is not over 20% using SBX as collector with a dosage of 220 mg/L. The recovery increases as the dosage increases in the range of 0 to 220 mg/L. When the dosage is more than 220 mg/L, the recovery begins to decline. This phenomenon is consistent with previous research findings [38]. According to the research findings of R. Liu et al., the corresponding sulfidization mechanism is that higher Na_2S concentration results in more sulfidization products on malachite to form a $\text{Cu}_2(\text{OH})_2\text{CO}_3$ /copper sulfide core-shell structure. However, when the Na_2S is excessive, the copper sulfide grown on malachite can block the further sulfidization of the unreacted core so that excess sulfide species could adsorb onto the surface of core-shell structure and depress the flotation of malachite by hindering the adsorption of the collector [39].

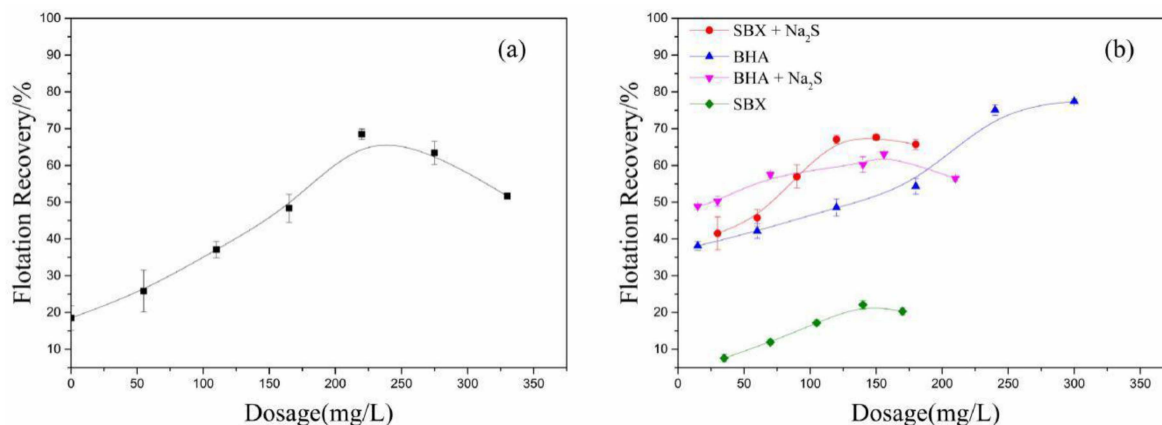


Figure 3. (a) Effect of Na₂S dosage on the recovery of malachite. The dosage of sodium butyl-xanthate (SBX) is 220 mg/L, pH = 9.5, the dosage of foaming agent is 40 mg/L. (b) Effect of dosage of SBX/ benzohydroxamic acid (BHA) on the recovery of malachite in the presence/absence of Na₂S. In the absence of Na₂S, pH is 9.5, and the dosage of terpenic oil is 40 mg/L. In the presence of Na₂S, pH is 9.5, the Na₂S dosage is 220 mg/L, and the dosage of terpenic oil is 40 mg/L. Terpenic oil is used as a foaming agent.

In the presence of Na₂S, the recovery of malachite increases from 50% to 63% as the dosage of BHA increases from 15 to 160 mg/L. In the absence of Na₂S, the recovery of malachite increases from 40% to 50% in the same range as that of the BHA dosage. This indicates that the addition of Na₂S increases the recovery of malachite by about 12% when using BHA as a collector. More significantly, in the same range as that of the SBX dosage, the addition of Na₂S increases the recovery of malachite by over 30% when using SBX as a collector. These phenomena should be attributed to the fact that the adsorption of sulfide ions improves the hydrophobicity of the malachite surface.

It should be mentioned that the recovery of malachite is over 60% when using BHA as a collector with a dosage of 220 mg/L in the absence of Na₂S, but the recovery is below 20% when using SBX as collector with the same dosage. This suggests that SBX could not adsorb well onto the unsulfurized surface, but BHA could adsorb well onto the unsulfurized surface. Particularly, after adding Na₂S, the recovery of malachite is over 65% when using SBX as a collector with the same dosage; it is increased by over 45% compared to without Na₂S. This suggests that SBX could adsorb well onto the sulfurized surface. Based on the above analysis, the proposed basic assumption was that the sulfide mineral collector (sodium butyl-xanthate) could interact well with the sulfurized zone and the oxide mineral collector (benzohydroxamic acid) could interact well with unsulfurized zone. Accordingly, malachite flotation tests using SBX and BHA as a combined collector were performed under the same conditions. Table 1 summarizes the flotation recovery of malachite using the combined collector with different molar ratios. As shown in Table 1, the recovery of malachite by using the combined BHA and SBX is significantly higher than that when they are used alone. Particularly, as shown in Figure 4, when the molar ratio of SBX and BHA is 3:1, the recovery of malachite reaches the maximum of about 90%. It is increased by over 30% compared to when they are used alone. Therefore, BHA and SBX have an obvious synergistic effect on the sulfidization flotation process [26].

3.2. Zeta-Potential Measurements

It is well known that the change in the charge on a mineral surface is closely related to the adsorption of the flotation reagents. The results of the zeta-potential measurements for malachite as a function of pH, in the presence and absence of flotation reagents, are presented in Figure 5. One can see that the isoelectric point (IEP) of the studied malachite surface has a pH value of 8.5, which is consistent with the reported IEP of malachite, i.e., 8–8.5 [17,40]. After adding the flotation reagents, the zeta potential of the malachite surface becomes more negative in the tested pH range, which is consistent with the phenomenon

observed by Feng [3]. When SBX and BHA are used as a combined collector, the zeta potential is more negative than that when SBX and BHA are used alone. This suggests that the anionic collectors of BHA and SBX are synergistically adsorbed on the surface of malachite, resulting in a significant decrease of the zeta potential of the malachite surface.

Table 1. The flotation recovery of malachite by using SBX, BHA, and their mixture (the total dosage of SBX + BHA is 180 mg/L).

BHA (mg/L)	Recovery/%	SBX (mg/L)	Recovery/%	SBX: BHA	Recovery/%
0	36.9	360	24.4	180:0	58.7
90	53.5	270	56.4	135:45	87.2
120	55.0	240	57.8	120:60	82.2
180	54.9	180	58.7	90:90	75.6
240	60.2	120	67.1	60:120	70.0
270	51.0	90	53.0	45:135	67.8
360	42.6	0	36.9	0:180	54.9

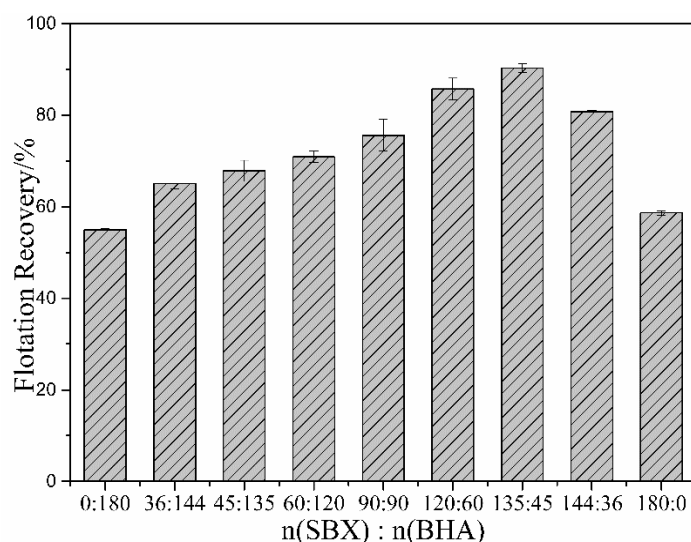


Figure 4. Effect of the molar ratio of SBX and BHA on flotation recovery. The dosage of Na_2S is 220 mg/L, pH = 9.5, and the total dosage of SBX with BHA is 180 mg/L.

3.3. FTIR Tests

As shown in Figure 6, the band around 1509 cm^{-1} should be ascribed to the stretching vibration of the C=O bond of the $-\text{CO}_3$ group on the malachite surface, the band around 1409 cm^{-1} should correspond to the stretching vibration peak of the C-O bond of the $-\text{CO}_3$ group on the malachite surface, and the band around 3400 cm^{-1} should be ascribed to the stretching vibration of -OH. The adsorption band around 2973 cm^{-1} in the FTIR spectrum of SBX should be ascribed to the stretching vibration peak of the C-H bond. The characteristic band around 1060 cm^{-1} is the stretching vibration of the C=S bond of SBX, and the band around 1109 cm^{-1} corresponds to the stretching vibration of C-O-C of SBX [26]. The 3393 cm^{-1} in the FTIR spectrum of SBX should be attributed to the characteristic peak of the stretching vibration of O-H of the water molecules adsorbed onto SBX. In the spectral line of BHA, the 1165 cm^{-1} should be ascribed to the stretching vibration peak of the C-O bond in the isomer of BHA. The 1489 cm^{-1} is the characteristic peak of the benzene ring skeleton of BHA, and the peak at 1653 cm^{-1} is the characteristic peak of the C-N bond of BHA [41]. Compared with the spectrum of the pure malachite mineral, there are new peaks in the spectrum of malachite treated with the mixed collector and Na_2S . It is very interesting to find that the peaks around 2973 cm^{-1} should be the corresponding characteristic absorption peaks of the C-H bond stretching vibration of SBX, the peak at 1623 cm^{-1} should be the C-N bond stretching vibration peak of BHA, and the

new peak at 1186 cm^{-1} should be ascribed to the combined effect of the C-O-C stretching vibration of SBX and the C-O stretching vibration of BHA [42]. The characteristic peaks of BHA and SBX in the FTIR spectrum of malachite treated by the mixed collector of BHA and SBX confirm that the two collectors can chemically adsorb onto the surface of malachite simultaneously.

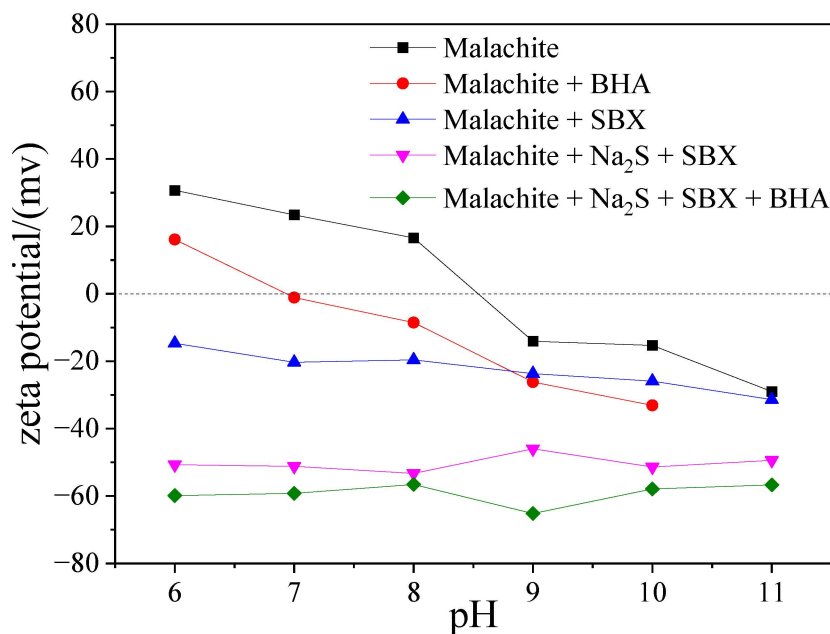


Figure 5. Zeta potential of malachite before and after the treatment with BHA, SBX, and their mixtures.

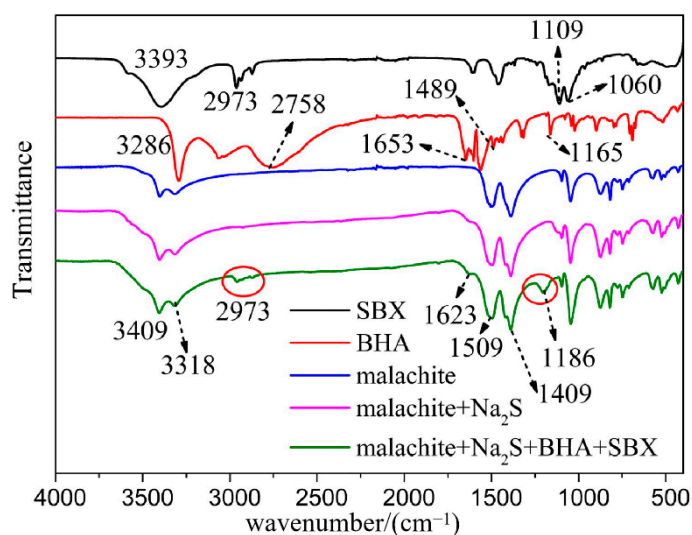


Figure 6. Infrared spectra of malachite before and after the treatment of the mixed collector and Na_2S , and the infrared spectra of BHA and SBX.

3.4. Raman Spectroscopy Tests

The Raman spectra of BHA, SBX, and malachite before and after the treatment with Na_2S and the mixed collectors are shown in Figure 7. It is obvious that the Raman peaks of malachite change dramatically before and after the collector treatment. As shown in Figure 7a, the peaks at 253 cm^{-1} and 327 cm^{-1} should be ascribed to the Raman characteristic peaks of the bond of Cu-O in the Raman spectrum of the pure malachite mineral [43]. After treatment by Na_2S , a new peak appears at 472 cm^{-1} , which should be ascribed to

the Raman characteristic peak of the bond of Cu-S. These results suggest that the chemical adsorption of Na_2S onto the surface could lead to the formation of a Cu-S bond on the surface of the malachite.

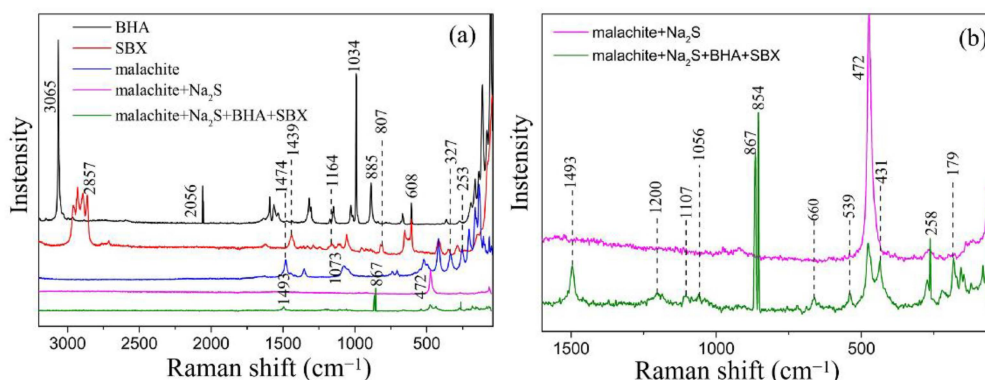


Figure 7. Raman spectra of BHA, SBX, and malachite before and after the treatment with Na_2S and mixed collectors. (a) The range of Raman spectra is from 40 to 3250 cm^{-1} . (b) The range of Raman spectra is from 40 to 1600 cm^{-1} .

After treatment by Na_2S and the mixed collectors, the peaks at 472 cm^{-1} and 431 cm^{-1} appear in the Raman spectrum; the peak at 472 cm^{-1} should be attributed to the Raman characteristic peak of the Cu-S bond resulting from the reaction of Na_2S with the surface of malachite, and the peak at 431 cm^{-1} should be ascribed to the Raman characteristic peak of the Cu-S bond resulting from the reaction of SBX with the surface of malachite.

The peak around 1493 cm^{-1} should be ascribed to the characteristic Raman peak of the $-\text{CH}_3$ anti-symmetrical deformation of SBX. The peak at 1034 cm^{-1} could be assigned to the characteristic peak of the benzene ring. In addition, affected by the surface, the characteristic peak of the benzene ring at 1034 cm^{-1} could move in the direction of a higher wavenumber; thus, the peak at 1056 cm^{-1} should be ascribed to the characteristic peak of the benzene ring in the green line (the Raman spectrum line of malachite treated by Na_2S and the mixed collectors) [44]. The Raman characteristic peak of the $-\text{CH}$ out-of-plane bend of BHA is located at 885 cm^{-1} [44], which shifts from the original 885 cm^{-1} to 867 cm^{-1} after adsorption onto the malachite surface, owing to the surface restriction. The above discussions indicate that SBX and BHA chemically adsorb onto the surface of malachite at the same time.

3.5. Computational Results

3.5.1. Surface Geometry Structure of Malachite

As shown in Figure 8, malachite is a monoclinic system with a layered structure. There is no bond between two adjacent layers, indicating that their interaction is weak. The crystal structure of each layer is symmetrical, possessing two types of copper atoms (denoted Cu1 and Cu2, respectively). The Mulliken population is a good representation of the distribution of charge between atoms. It can be utilized to analyze the charge distribution, charge transfer, and chemical bond properties of a given system [45]. The average Mulliken populations of the Cu, O, C, and H atoms in the crystal structure of the malachite surface are listed in Table 2. Obviously, copper atoms possess more positive charge, suggesting that copper atoms could potentially become the active sites for the adsorption of an anion reagent.

According to the previous literature [10] and the XRD results, the (-201) surface is a crystal dissociation surface with a complete structure, and its surface energy is relatively low. Accordingly, the optimized primitive cell of malachite was initially cleaved crossing the (-201) crystal plane at the top position of -0.68 with 3.0 thickness in the fractional coordination. Then, a slab with a vacuum region of at least 20 Å was built to construct a surface slab model of malachite. The optimized (-201) surface of malachite is shown in Figure 9.

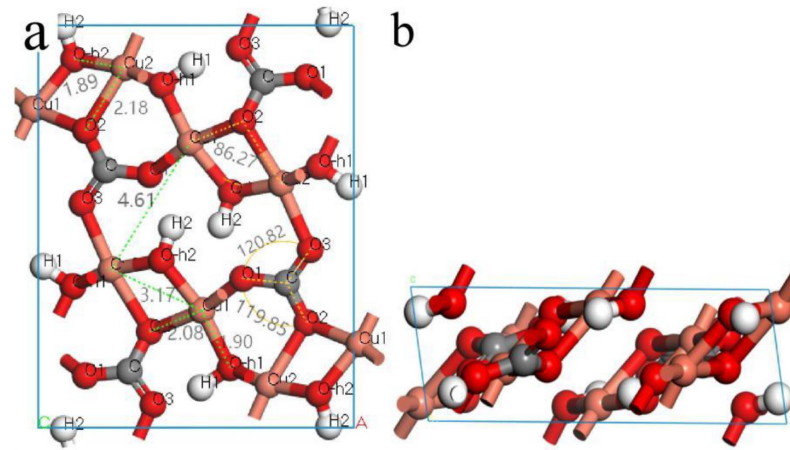


Figure 8. Malachite unit cell of the optimized structural model: (a) top view; (b) lateral view.

Table 2. Mulliken populations of various atoms on malachite's surface.

Atom	Atomic Orbital Layout			Total(e)	Electric Charge(e)
	s	p	d		
C	0.86	2.38	0.00	3.24	0.76
O	1.83	4.85	0.00	6.68	−0.68
Cu	0.44	0.16	9.43	10.03	0.97
H	0.63	0.00	0.00	0.63	0.37

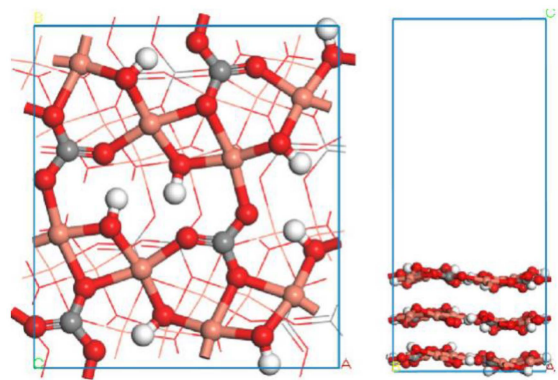


Figure 9. Optimized (−201) surface of malachite: (left) top view; (right) lateral view. The balls in orange, red, gray, and white colors represent copper atoms, oxygen atoms, carbon atoms, and hydrogen atoms, respectively.

3.5.2. Molecular Geometry Structures of Flotation Reagents

The relevant chemical reactivity of a given molecule can be well interpreted by using the frontier molecular orbitals (HOMO and LUMO) [46]. HOMO determines the capacity of a molecule to donate electrons and the spatial distribution of valence electrons, which mainly participate in the formation of chemical bonds, and LUMO is closely correlated with the capacity of a molecule to accept electrons.

Figure 10 presents the HOMO and LUMO of (a) SBX and (b) BHA. It is demonstrated that the HOMO and LUMO of SBX are mainly distributed in the dithiocarbonate group (−OCS₂), and the HOMO of BHA is mostly located at the chelation group (−CO-NH-O−). According to the electron distribution of the frontier molecular orbitals of BHA and SBX, it can be expected that the dithiocarbonate group (−OCS₂) in the SBX molecule could become the active site for possible reactions, and the chelation group (−CO-NH-O−) in the BHA molecule could offer the possible active sites.

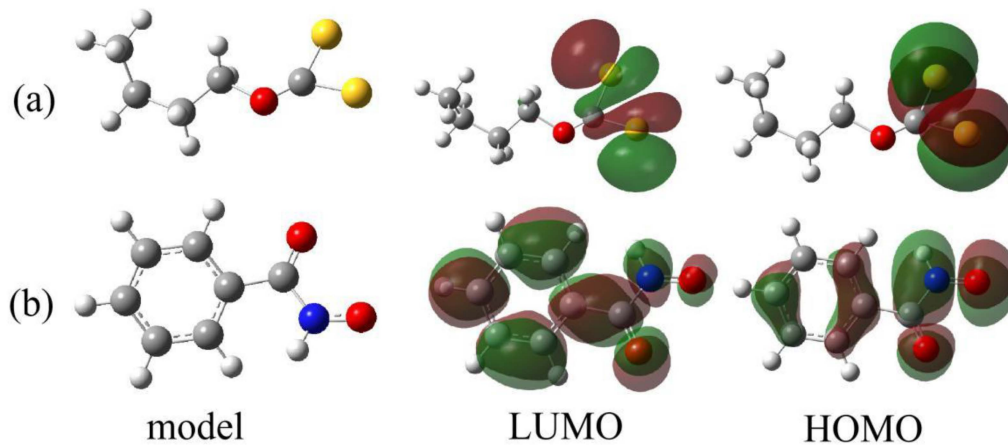


Figure 10. Optimized structural models of (a) SBX and (b) BHA with their frontier molecular orbitals: highest occupied molecular orbital (HOMO) and lowest unoccupied molecular orbital (LUMO). The molecular models and molecular orbitals of SBX and BHA were rendered by using Gaussview 5.0 software. The balls in gray, red, yellow, blue, and white colors represent carbon atoms, oxygen atoms, sulfur atoms, nitrogen atoms, and hydrogen atoms, respectively.

3.5.3. Adsorption of Flotation Reagents onto the (−201) Surface of Malachite

In order to further study the synergistic mechanism, a series of mineral surface models were constructed to demonstrate the adsorption configuration of pharmaceutical molecules on malachite's surface. The adsorption energies of the adsorbates on the mineral surface were calculated with the following equation:

$$\Delta E_{\text{ads}} = E_{\text{surface+adsorbates}} - E_{\text{surface}} - E_{\text{adsorbates}}, \quad (1)$$

where ΔE_{ads} represents the adsorption energy, $E_{\text{surface+adsorbates}}$ refers to the total energy adsorbed onto the mineral surface of the following structural optimization, E_{surface} represents the total energy of the malachite surface without the adsorbate, and $E_{\text{adsorbate}}$ is the adsorbate energy. The adsorption energies of adsorbates on the surface of malachite are given in Table 3.

Table 3. Adsorption energies of adsorbates on the surface of malachite.

Systems	Adsorption Energy of Various Reagents (kcal/mol)
SBX	−8.9
BHA	−8.7
BHA + SBX after sulfuration	−72.8
SBX after sulfuration	−51.9
BHA after sulfuration	−39.0
S^{2-}	−49.3
H_2O	−5.9
SH^-	−19.9
OH^-	−28.7

As shown in Figure 11, for malachite, the active sites in the surface are mainly Cu atoms, which is consistent with the Mulliken population analysis. In addition, S^{2-} , SH^- , OH^- , and H_2O can be adsorbed onto the surface of minerals. According to the solution chemistry, there are mainly S^{2-} and SH^- in the pulp during the vulcanization process. The optimized surface structure shows that the bond length of the Cu-S bond by SH^- is longer than that on the surface of malachite, and the adsorption energy of S^{2-} on the surface of malachite is significantly lower than that of SH^- , which indicates that the adsorption of S^{2-} onto the surface is more favorable in thermodynamics. Therefore, S^{2-} is used as the main active component in the subsequent calculations. The adsorption energy of OH^- is more negative than that of H_2O , which indicates that in an alkaline environment, OH^-

could be easily adsorbed onto the surface of malachite, enhancing the hydrophilicity of the malachite surface and hindering the adsorption of the collector. The adsorption energies of S^{2-} and OH^- are -49.3 kcal/mol and -28.7 kcal/mol, respectively. This suggests that S^{2-} possesses a strong driving force to replace OH^- and then to be adsorbed onto the malachite surface in thermodynamics. As shown in Figure 11i–l, the adsorption configuration of SBX onto the malachite surface before and after sulfurization is significantly different. Before sulfurization, the sulfur atoms of SBX are respectively bonded to Cu atoms on the malachite surface, resulting in the formation of two Cu-S bonds in the surface with bond lengths of 2.46 Å and 2.48 Å. After sulfurization, SBX and Cu are connected by an S atom to form a '(S-S-Cu)_{1 layer}-O_{2 layer}' adsorption configuration with a S-S bond length of 2.05 Å. Interestingly, one Cu-O bond in the first layer of the malachite surface model is broken, and the Cu atom forms a new Cu-O bond with the oxygen atom in the second layer, resulting in a new quaternary coordination structure of the Cu ion with a Cu-S bond length of 2.26 Å. Obviously, the adsorption of xanthate on the vulcanized surface of malachite causes surface reconstruction and promotes the interaction between surface layers. The calculated results also indicate that the adsorption energy of xanthate on the vulcanized surface is -51.9 kcal/mol, which is much lower than that on the unvulcanized surface, with a value of -8.9 kcal/mol.

In addition, as shown in Figure 11m–p, BHA is mainly adsorbed onto the unvulcanized site of the malachite surface after sulfurization. The bond length (1.99 Å) formed by BHA on the vulcanized surface is shorter than that (2.88 Å) formed by BHA on the unvulcanized surface. The adsorption energy of -39.0 kcal/mol is also much more negative than that before sulfurization, with a value of -8.7 kcal/mol. These results consistently demonstrate that BHA could be more strongly adsorbed onto the vulcanized surface.

In particular, as shown in Figure 11s,t, the synergistic adsorption of SBX and BHA onto the vulcanized surface promotes the interlayer interaction of the malachite surface with the formation of a Cu-O bond between surface layers. When the two reagents are adsorbed onto the surface of malachite, it can be seen that BHA is adsorbed on the unvulcanized copper active site, while SBX is adsorbed onto the vulcanized active site with S^{2-} as the bridge. The adsorption energy of SBX and BHA on the malachite surface is -72.8 kcal/mol, which is much lower than that by SBX (-8.9 kcal/mol) or BHA (-8.7 kcal/mol) alone. In addition, it was found that an intermolecular hydrogen bond formed between BHA and SBX. Accordingly, the synergistic effect from the co-adsorption, hydrogen bonds, and Van der Waals interactions of SBX and BHA on the malachite greatly promotes the flotation recovery of malachite.

It should be mentioned that the simplified surface model in vacuum was just used in this work to qualitatively explain the synergistic adsorption mechanism of SBX and BHA on the malachite surface owing to the complexity of the flotation interface structure. The effects of water molecules were ignored here based on the fact that the adsorption of water molecules onto the surface is relatively weak (only -5.9 kcal/mol) and almost cannot change the adsorption behavior of the flotation reagent. At the same time, a large amount of computational cost could be saved, and the calculation of the model became more efficient.

It should be emphasized that this work was focused on the better performance of the combined collectors of BHA and SBX than the collectors BHA or SBX alone, and the electrochemical properties of vulcanized malachite surfaces were not considered in all flotation tests in this study. The effects of the electrochemical potential environment on the adsorption of collector are indeed important. They are worth further investigating in future.

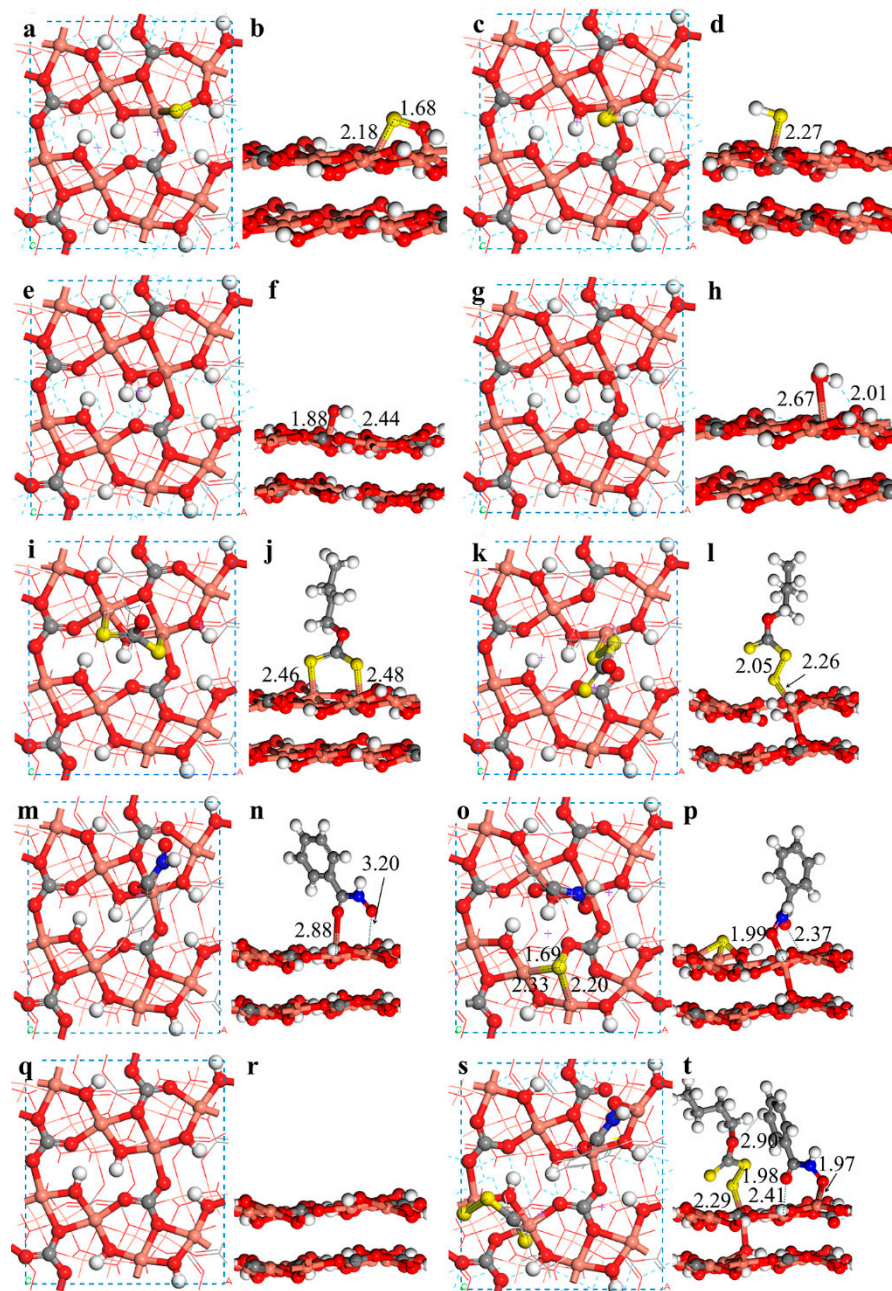


Figure 11. The adsorption model of the malachite surface in the absence of water molecules; (a) and (b) are the side and top views of the S^{2-} adsorbed malachite surface, respectively; (c) and (d) are the side and top views of the adsorption of SH^{-} onto the malachite surface; (e) and (f) are the side and top views of the adsorption of OH^{-} onto the malachite surface; (g) and (h) are the side and top views of the adsorption of water molecules onto the malachite surface; (i) and (j) are the side and top views of the adsorption of SBX onto the malachite surface; (k) and (l) are the side and top views of the adsorption of SBX onto the S^{2-} adsorbed malachite surface; (m) and (n) are the side and top views of the adsorption of BHA onto the surface of malachite; (o) and (p) are the side and top views of the adsorption of BHA onto the S^{2-} adsorbed malachite surface; (q) and (r) are the optimized (-201) surface of malachite; (s) and (t) are the side and top views of the co-adsorption of BHA and SBX onto the malachite surface (the balls in orange, red, gray, white, yellow, and blue colors represent copper atoms, oxygen atoms, carbon atoms, hydrogen atoms, sulfur atoms, and nitrogen atoms, respectively).

4. Conclusions

In this work, when SBX and BHA were mixed with a molar ratio of 3:1, the recovery of malachite reached 90%, possessing a much higher recovery—by about 20%—than only using SBX. The zeta-potential test results showed that the surface potential of malachite decreased due to the adsorption of collector ions onto the surface in the studied pH range. At the same time, the characteristic adsorption peaks of SBX and BHA appeared in FTIR and Raman spectra, indicating that SBX and BHA ions were chemically adsorbed onto the malachite surface. The DFT calculation results further indicated that the co-adsorption energy (−72.8 kcal/mol) of SBX with BHA was much lower than that of only BHA (−8.7 kcal/mol) or SBX (−8.9 kcal/mol), confirming the synergistic adsorption of SBX and BHA onto the surface. Finally, a synergistic adsorption model was proposed on the vulcanized surface of malachite. This work shed some new light on the design and development of more efficient combined flotation reagents.

Author Contributions: The manuscript was written through contributions of all authors. W.S. and B.H. conceived and designed the experiments; C.Z. designed the calculations; Q.Z. and C.Z. performed experiments and wrote the original paper; B.A. investigated the literature and did spectroscopy tests; T.Y. and S.C. analyzed the experimental data and modified the paper; B.H. and M.L. performed flotation tests; C.Z. and Q.Z. performed the DFT calculations and analyzed the computational results; J.H. drew the figures; J.Z. and D.C. analyzed the flotation results and revised the paper. All authors have read and agreed to the published version of the manuscript.

Funding: This work was funded by the National Key Research and Development Program of China, grant number 2019YFC0408303; the Natural Science Foundation of China, grant number 51704330, 52074356 and U20A20269; the Natural Science Foundation of Hunan Province, grant number 2020JJ5759; China Postdoctoral Science Foundation, grant number 2020T130188 and 2018M642988; the Fundamental Research Funds for the Central Universities of Central South University, grant number 2020zzts737; the Training Program for Distinguished Innovative Youth of Changsha, grant number kq2009005; the National 111 Project, grant number B14034; the Collaborative Innovation Center for Clean and Efficient Utilization of Strategic Metal Mineral Resources.

Institutional Review Board Statement: Not applicable.

Informed Consent Statement: Not applicable.

Data Availability Statement: The data presented is available in the article.

Acknowledgments: This work was financially supported by the National Key Research and Development Program of China (2019YFC0408300); the Natural Science Foundation of China (No. 51704330; No. 52074356; U20A20269); the Natural Science Foundation of Hunan Province (No. 2020JJ5759); China Postdoctoral Science Foundation (No.2020T130188, No. 2018M642988); the Fundamental Research Funds for the Central Universities of Central South University [No.2020zzts737]; the Training Program for Distinguished Innovative Youth of Changsha (kq2009005); the National 111 Project (No. B14034); the Collaborative Innovation Center for Clean and Efficient Utilization of Strategic Metal Mineral Resources.

Conflicts of Interest: The authors declare no conflict of interest. The funders had no role in the design of the study; in the collection, analyses, or interpretation of data; in the writing of the manuscript, or in the decision to publish the results.

References

1. Wu, D.; Ma, W.; Mao, Y.; Deng, J.; Wen, S. Enhanced sulfidation xanthate flotation of malachite using ammonium ions as activator. *Sci. Rep.* **2017**, *7*, 2086. [[CrossRef](#)] [[PubMed](#)]
2. Deng, J.-S.; Wen, S.-M.; Deng, J.-Y.; Wu, D.-D. Extracting copper from copper oxide ore by a zwitterionic reagent and dissolution kinetics. *Int. J. Miner. Metall. Mater.* **2015**, *22*, 241–248. [[CrossRef](#)]
3. Feng, Q.; Zhao, W.; Wen, S.; Cao, Q. Copper sulfide species formed on malachite surfaces in relation to flotation. *J. Ind. Eng. Chem.* **2017**, *48*, 125–132. [[CrossRef](#)]
4. Hope, G.A.; Buckley, A.N.; Parker, G.K.; Numprasanthai, A.; Woods, R.; McLean, J. The interaction of n-octanohydroxamate with chrysocolla and oxide copper surfaces. *Miner. Eng.* **2012**, *36–38*, 2–11. [[CrossRef](#)]

5. Liu, C.; Zhu, G.; Song, S.; Li, H. Interaction of gangue minerals with malachite and implications for the sulfidization flotation of malachite. *Colloid Surf. A Physicochem. Eng. Asp.* **2018**, *555*, 679–684. [[CrossRef](#)]
6. Feng, Q.; Zhao, W.; Wen, S. Surface modification of malachite with ethanediamine and its effect on sulfidization flotation. *Appl. Surf. Sci.* **2018**, *436*, 823–831. [[CrossRef](#)]
7. Mao, Y.B.; Deng, J.S.; Wen, S.M.; Fang, J.J. Reaction kinetics of malachite in ammonium carbamate solution. *Chem. Pap.* **2015**, *69*, 1187–1192. [[CrossRef](#)]
8. Marion, C.; Jordens, A.; Li, R.; Rudolph, M.; Waters, K.E. An evaluation of hydroxamate collectors for malachite flotation. *Sep. Purif. Technol.* **2017**, *183*, 258–269. [[CrossRef](#)]
9. Lebernegg, S.; Tsirlin, A.A.; Janson, O.; Rosner, H. Spin gap in malachite $\text{Cu}_2(\text{OH})_2\text{CO}_3$ and its evolution under pressure. *Phys. Rev. B* **2013**, *88*. [[CrossRef](#)]
10. Wu, D.; Mao, Y.; Deng, J.; Wen, S. Activation mechanism of ammonium ions on sulfidation of malachite (–201) surface by DFT study. *Appl. Surf. Sci.* **2017**, *410*, 126–133. [[CrossRef](#)]
11. Li, G. Study on the Mechanism of Ammonium (Amine) Salt in Sulfide Flotation of Copper Ore. Master's Thesis, Kunming University of Science and Technology, Kunming, China, 2017.
12. Liu, C.; Feng, Q.; Zhang, G. Effect of ammonium sulfate on the sulfidation flotation of malachite. *Arch. Min. Sci.* **2018**, *63*, 139–148. [[CrossRef](#)]
13. Li, M.; Liu, J.; Hu, Y.; Gao, X.; Yuan, Q.; Zhao, F. Investigation of the specularite/chlorite separation using chitosan as a novel depressant by direct flotation. *Carbohydr. Polym.* **2020**, *240*, 116334. [[CrossRef](#)] [[PubMed](#)]
14. Barbaro, M.; Urbina, R.H.; Cozza, C.; Fuerstenau, D.; Marabini, A. Flotation of oxidized minerals of copper using a new synthetic chelating reagent as collector. *Int. J. Miner. Process.* **1997**, *50*, 275–287. [[CrossRef](#)]
15. Choi, J.; Choi, S.Q.; Park, K.; Han, Y.; Kim, H. Flotation behaviour of malachite in mono- and di-valent salt solutions using sodium oleate as a collector. *Int. J. Miner. Process.* **2016**, *146*, 38–45. [[CrossRef](#)]
16. Jiang, T.; Fang, J.; Mao, Y.; Li, G.; Bi, K. Impact of ammonium (amine) salts on behavior of malachite sulfide flotation. *Conserv. Util. Miner. Resour.* **2015**, *3*, 31–37. [[CrossRef](#)]
17. Liu, C. Study and Application of Sulfide Flotation of Malachite from Typical Copper Oxide Ores. Master's Thesis, Jiangxi University of Science and Technology, Ganzhou, China, 2012.
18. Naklicki, M.L.; Rao, S.R.; Gomez, M.; Finch, J.A. Flotation and surface analysis of thenickel oxide amyl xanthate system.pdf. *Int. J. Miner. Process.* **2002**, *65*, 73–82. [[CrossRef](#)]
19. Lee, K.; Archibald, D.; McLean, J.; Reuter, M.A. Flotation of mixed copper oxide and sulphide minerals with xanthate and hydroxamate collectors. *Miner. Eng.* **2008**, *22*, 395–401. [[CrossRef](#)]
20. Fuxing, Y.; Peilun, L.; Chengxing, W.; Baoxu, S. Research on flotation process for a refractory copper oxide ore. *Min. Process. Equip.* **2014**, *42*, 109–113. [[CrossRef](#)]
21. Castro, S.; Soto, H.; Goldfarb, J.; Laskowski, J. Sulphidizing reactions in the flotation of oxidized copper minerals, II. Role of the adsorption and oxidation of sodium sulphide in the flotation of chrysocolla and malachite. *Int. J. Miner. Process.* **1974**, *1*, 151–161. [[CrossRef](#)]
22. Yujun, F.; Xiuyun, J. Several problem of oxide copper sulphidizing flotation. *Shanxi Metall.* **2004**, *2*. [[CrossRef](#)]
23. Liu, C.; Zhang, W.; Song, S.; Li, H.; Jiao, X. A novel insight of the effect of sodium chloride on the sulfidization flotation of cerussite. *Powder Technol.* **2019**, *344*, 103–107. [[CrossRef](#)]
24. Gao, Z.; Bai, D.; Sun, W.; Cao, X.; Hu, Y. Selective flotation of scheelite from calcite and fluorite using a collector mixture. *Miner. Eng.* **2015**, *72*, 23–26. [[CrossRef](#)]
25. Tian, J.; Xu, L.; Deng, W.; Jiang, H.; Gao, Z.; Hu, Y. Adsorption mechanism of new mixed anionic/cationic collectors in a spodumene-feldspar flotation system. *Chem. Eng. Sci.* **2017**, *164*, 99–107. [[CrossRef](#)]
26. Yin, W.-Z.; Sun, Q.-Y.; Li, D.; Tang, Y.; Fu, Y.-F.; Yao, J. Mechanism and application on sulphidizing flotation of copper oxide with combined collectors. *Trans. Nonferrous Met. Soc. China* **2019**, *29*, 178–185. [[CrossRef](#)]
27. Deng, J.-S.; Wen, S.-M.; Liu, J.; Wu, D.-D.; Feng, Q.-C. Adsorption and activation of copper ions on chalcopyrite surfaces: A new viewpoint of self-activation. *Trans. Nonferrous Met. Soc. China* **2014**, *24*, 3955–3963. [[CrossRef](#)]
28. Tian, M.; Liu, R.; Gao, Z.; Chen, P.; Han, H.; Wang, L.; Zhang, C.; Sun, W.; Hu, Y. Activation mechanism of Fe (III) ions in cassiterite flotation with benzohydroxamic acid collector. *Miner. Eng.* **2018**, *119*, 31–37. [[CrossRef](#)]
29. Vagenas, N. Quantitative analysis of synthetic calcium carbonate polymorphs using FT-IR spectroscopy. *Talanta* **2003**, *59*, 831–836. [[CrossRef](#)]
30. Wang, Y.; Li, H.; Chen, J.; Gao, R. Progress in the application of raman spectroscopy to water quality analysis. *Earth Environ.* **2014**, *42*, 260–264. [[CrossRef](#)]
31. Cong, X.; Liu, X.-L.; Lin, M.-L.; Tan, P.-H. Application of Raman spectroscopy to probe fundamental properties of two-dimensional materials. *NPJ 2D Mater. Appl.* **2020**, *4*, 981–1013. [[CrossRef](#)]
32. Uusitalo, S.; Soudunsaari, T.; Sumen, J.; Haavisto, O.; Kaartinen, J.; Huuskonen, J.; Tuikka, A.; Rahkamaa-Tolonen, K.; Paaso, J. Online analysis of minerals from sulfide ore using near-infrared Raman spectroscopy. *J. Raman Spectrosc.* **2020**, *51*, 978–988. [[CrossRef](#)]
33. Downs, R.T.; Hall-Wallace, M. The American mineralogist crystal structure database. *Am. Mineral.* **2003**, *88*, 247–250.

34. Clark, S.J.; Segall, M.D.; Pickard, C.J.; Hasnip, P.J.; Probert, M.I.J.; Refson, K.; Payne, M.C. First principles methods using CASTEP. *Z. Krist. Cryst. Mater.* **2005**, *220*, 567–570. [[CrossRef](#)]
35. Cui, W.; Song, X.; Chen, J.; Chen, Y.; Li, Y.; Zhao, C. Adsorption behaviors of different water structures on fluorapatite (001) surface: A DFT study. *Front. Mater.* **2020**, *7*. [[CrossRef](#)]
36. Liu, J.; Wen, S.; Deng, J.; Chen, X.; Feng, Q. DFT study of ethyl xanthate interaction with sphalerite (110) surface in the absence and presence of copper. *Appl. Surf. Sci.* **2014**, *311*, 258–263. [[CrossRef](#)]
37. Yu, H.S.; Li, S.L.; Truhlar, D.G. Perspective: Kohn-Sham density functional theory descending a staircase. *J. Chem. Phys.* **2016**, *145*, 130901. [[CrossRef](#)] [[PubMed](#)]
38. Liu, R.; Liu, D.; Li, J.; Li, J.; Liu, Z.; Jia, X.; Yang, S.; Li, J.; Ning, S. Sulfidization mechanism in malachite flotation: A heterogeneous solid-liquid reaction that yields Cu_xS_y phases grown on malachite. *Miner. Eng.* **2020**, *154*. [[CrossRef](#)]
39. Xing, C. Discussion on Mechanism of Catalytic Oxidation of Ammonium Salt-Malachite-Sodium Sulfide System. Master's Thesis, Kunming University of Science and Technology, Kunming, China, 2012.
40. Li, Z.; Rao, F.; Guo, B.; Zuo, W.; Song, S.; López-Valdivieso, A. Effects of calcium ions on malachite flotation with octyl hydroxamate. *Miner. Eng.* **2019**, *141*. [[CrossRef](#)]
41. Cao, Y.; Sun, L.; Gao, Z.; Sun, W.; Cao, X. Activation mechanism of zinc ions in cassiterite flotation with benzohydroxamic acid as a collector. *Miner. Eng.* **2020**, *156*. [[CrossRef](#)]
42. Qingbo, M.; Xiaoping, X.; Yude, G.; Guosheng, W. Influence of combined use of sodium octyl hydroxamate acid and butyl xanthate on flotation behavior of malachite. *Metal. Mine* **2018**, *6*, 70–74. [[CrossRef](#)]
43. Zhang, Q.; Zhang, K.; Xu, D.; Yang, G.; Huang, H.; Nie, F.; Liu, C.; Yang, S. CuO nanostructures: Synthesis, characterization, growth mechanisms, fundamental properties, and applications. *Prog. Mater. Sci.* **2014**, *60*, 208–337. [[CrossRef](#)]
44. Guo, B.; Lin, X.; Burgess, I.J.; Yu, C. Electrochemical SHINERS investigation of the adsorption of butyl xanthate and 2-mercaptobenzothiazole on pyrite. *Appl. Surf. Sci.* **2020**, *529*, 147118. [[CrossRef](#)]
45. Segall, M.D.; Shah, R.; Pickard, C.J.; Payne, M.C. Population analysis of plane-wave electronic structure calculations of bulk materials. *Phys. Rev. B* **1996**, *54*, 16317–16320. [[CrossRef](#)] [[PubMed](#)]
46. Chen, P.; Hu, Y.; Gao, Z.; Zhai, J.; Fang, D.; Yue, T.; Zhang, C.; Sun, W. Discovery of a novel cationic surfactant: Tributyltetradecylphosphonium chloride for iron ore flotation: From prediction to experimental verification. *Minerals* **2017**, *7*, 240. [[CrossRef](#)]